Noname manuscript No.
(will be inserted by the editor)

An improved soft-kill BESO algorithm for optimal distribution of single or multiple material phases

Kazem Ghabraie

the date of receipt and acceptance should be inserted later

Abstract Finding the optimum distribution of material phases in a multi-material structure is a frequent and important problem in structural engineering which involves topology optimization. The Bi-directional Evolutionary Structural Optimization (BESO) method is now a well-known topology optimization method. In this paper an improved soft-kill BESO algorithm is introduced which can handle both single and multiple material distribution problems. A new filtering scheme and a gradual procedure inspired by the continuation approach are used in this algorithm. Capabilities of the proposed method are demonstrated using different examples. It is shown that the proposed method can result in considerable improvements compared to the normal BESO algorithm particularly when solving problems involving very soft material or void phase.

Keywords Topology optimization · Gradual BESO · Multi-material design · Continuation approach · Soft-kill BESO

1 Introduction

In many cases in structural engineering, one needs to find the optimum distribution of one material within a medium filled with other materials. In structural optimization, such problems are translated into topology optimization problems.

The first widely used numerical topology optimization method for continua was introduced by Bendsøe and Kikuchi (1988) and is now commonly known as the *homogenization method*. Since then, topology optimization area attracted many researchers from different fields. During the last two decades, several new topology optimization methods were introduced, developed and their application in a wide range of physical problems was studied (Deaton and Grandhi 2014).

The central idea of the homogenization method is to convert the topology optimization problem to a large sizing optimization problem by defining topology as *material distribution*. Many of the well-known topology optimization methods adopted the material distribution approach. This includes Solid Isotropic Microstructures with Penalization (SIMP) and Bi-directional Evolutionary Structural Optimization (BESO) methods.

In the SIMP method, the design variables (x) are relative densities which continuously vary between $x = 1$ representing solids and a very small positive number, $0 < x = x_{\min} \ll 1$, representing voids. The intermediate values ($x_{\min} < x < 1$) of design variables are penalized using a power-law interpolation scheme (Bendsøe 1989). The BESO method, on the other hand, uses binary design variables with $x \in \{0, 1\}$. Because of its binary nature no penalization is required in this method.

The BESO method was originally introduced by Querin et al (1998) and Yang et al (1999) as a successor of the Evolutionary Structural Optimization (ESO) method which was proposed by Xie and Steven (1993). After discretizing the design domain using finite element method, to evolve the structure towards an optimal topology, BESO iteratively introduces new elements to efficient parts of the design domain and removes its inefficient elements.

BESO-type algorithms can be divided into two classes: hard-kill and soft-kill approaches. In single material distribution problems, the hard-kill approach is more common. In this approach the void elements are simply removed from the structure. In the soft-kill approach, on the other hand, the voids are replaced by a weak mate-

School of Civil Engineering and Surveying, University of Southern Queensland, Toowoomba QLD 4350, Australia
E-mail: kazem.ghabraie@usq.edu.au

rial. The soft-kill approach is essentially more suitable for multi-material problems.

Topology optimization methods were originally used for single material/void distribution problems. The first study in two-material distribution problems is published by Thomsen (1992) in which the homogenization method was employed. Sigmund and Torquato (1997) and Bendsøe and Sigmund (1999) extended the power-law material interpolation scheme in the SIMP method to more than two material phases. Later on the Discrete Material Optimization (DMO) method was proposed by Stegmann and Lund (2005) and Lund and Stegmann (2006) which extends the capabilities of the SIMP method to handle any number of possibly anisotropic materials. Apart from homogenization-based methods, different versions of level-set methods have also been introduced to solve multi-phase material distribution problems (see for example Zhou and Wang 2007; Wang and Wang 2004; Wang et al 2015). For other notable recent works in this area, the reader is referred to the works of Gao and Zhang (2011); Bruyneel (2011); Blasques and Stolpe (2012); Gao et al (2013); Tavakoli and Mohseni (2014); Tavakoli (2014); Park and Sutradhar (2015); Querin et al (2015).

Since its introduction, the BESO method was continually developed and applied to many different problems (Huang and Xie 2010). In multi-phase material distribution problems, the earliest application of the ESO method is published by Rispler and Steven (1995). Despite the apparent simplicity of using soft-kill BESO in two-phase material distribution problems, however, due to the numerical problems that are explained in section 2.5, this method was only recently used to solve these types of problems (see for example Liu et al 2008; Ghabraie 2009; Ghabraie et al 2010a,b; Nguyen et al 2014). Huang and Xie (2009) extended the BESO method to solve multi-phase material distribution problems.

This paper attempts to provide further improvements to the multi-material BESO algorithm proposed by Huang and Xie (2009). It focuses on proposing approaches to improve BESO results and treat the numerical anomalies which can arise when solving multi-material topology optimization problems with soft-kill BESO. Noting that single material design problems are special cases of multi-material design problems, the proposed approaches can be used in both single and multiple phase material distribution problems.

According to Sigmund and Petersson (1998), most topology optimization methods (including SIMP and BESO) are prone to three common numerical instabilities: mesh-dependency, formation of checkerboard patterns, and the local minima problem. Huang and Xie (2007) proposed a filtering scheme for hard-kill BESO which successfully eliminates checkerboard patterns and mesh dependency. This filtering scheme is introduced in section 2.5. Through a simple example in section 2.6, it is shown that this filtering scheme is not directly applicable to soft-kill BESO. A brief review of the treatment proposed by Huang and Xie (2009) for this problem is presented in section 3. Then a new filtering scheme is proposed in section 4 which works well with soft-kill BESO.

Topology optimization problems are generally not convex and have several local minima. Gradient based optimization techniques can be trapped in these local minima and miss the global optimum. As a result one may get different solutions by starting from different initial designs for the same problem. This is usually referred to as the local minima problem.

The so-called *continuation* approaches are used with the SIMP method to improve the final solutions and reduce their dependency on initial guess designs. These approaches initially solve an artificial convex (or near convex) version of the problem and then gradually change it back to the original problem. In section 5, a continuation approach is introduced which proves to be helpful in improving final solutions and obtaining the same solution for different initial designs in soft-kill BESO. The proposed improved BESO algorithm is tested using a number of examples in section 6.

2 BESO in multi-material distribution problem

2.1 Problem statement

Consider the following material distribution design problem with volume constraint

$$\begin{aligned} &\min_{\mathbf{x}\in\mathcal{X}^n} \quad f(\mathbf{x}) \\ &\text{such that} \quad V_i(\mathbf{x}) \le \bar{V}_i,\ i = 1,\dots,m-1, \end{aligned} \tag{1}$$

where $f : \mathcal{X}^n \mapsto \mathcal{R}$ is the objective function, V_i is the actual volume, and $\bar{V}_i$ is the maximum allowable volume for the i-th material phase in the design domain. n is the number of elements (design variables) and m is the number of material phases. $\mathbf{x} = [x_1, x_2, \dots, x_n]^T$ is the design variable vector. Using BESO, we can define $\mathcal{X} = \{0, 1, \dots, m-1\}$ which lists the possible values for any design variable.

Considering a two-material design problem ($m = 2$), in BESO each element can only have two states ($\mathcal{X} = \{0, 1\}$). For each element we use one design variable. $x_e = 0$ represents the first material phase for element e and $x_e = 1$ represents the second material phase for this element.

Consider a problem with two isotropic linear elastic material phases. For simplicity assume that the Poisson's ratios of the two material phases are equal. The two moduli of elasticity are $E^{(0)}$ and $E^{(1)}$. In its simplest form, elastic modulus of each element can be related to its design variable by the following linear interpolation scheme,

$$E_e(x_e) = E^{(0)} + x_e(E^{(1)} - E^{(0)}), \qquad e = 1, \ldots, n. \quad (2)$$

Without loss of generality, assume $E^{(1)} > E^{(0)}$.

The element level stiffness matrix $\mathbf{K}_e$ can be expressed as a function of E_e and consequently of x_e. The stiffness matrix of the system can be derived by assembling element stiffness matrices as follows

$$\mathbf{K}(\mathbf{x}) = \sum_{e=1}^{n} \mathbf{K}_e^g(x_e), \quad (3)$$

with $\mathbf{K}_e^g$ denoting the global level stiffness matrix of element e. The equilibrium equation can now be written as

$$\mathbf{K}(\mathbf{x})\mathbf{u} = \mathbf{f} \quad (4)$$

in which $\mathbf{f}$ and $\mathbf{u}$ are nodal load and displacement vectors respectively.

2.2 Sensitivity numbers

In the BESO method, the sensitivity number α_e is a measure of the effectiveness of changing the material phase of element e on reducing (or increasing in case of maximization) the objective function. Suppose that by changing the design variable value of the e-th element, the vector of design variables changes from $\mathbf{x}$ to $\mathbf{x}_e$. Based on Taylor series for f in the neighborhood of $\mathbf{x}_e$ we can obtain the following first-order approximation for the change in f due to changing x_e

$$\underset{e}{\Delta} f = f(\mathbf{x}_e) - f(\mathbf{x}) = \frac{\partial f}{\partial x_e}\Delta x_e. \quad (5)$$

The notation $\underset{e}{\Delta} f$ represents the effect of imposing a change in element e on the objective function and thus can be used to define the sensitivity number for the e-th element.

For a minimization problem, we can define the vector of sensitivity numbers to match the steepest descent search direction (Ghabraie 2009). This gives us the following sensitivity numbers

$$\alpha_e = -\frac{\partial f}{\partial x_e}, \quad e = 1, \ldots, n. \quad (6)$$

2.3 Minimum compliance design

Mean compliance is the most commonly used objective function in topology design of structures. It can be defined as

$$c(\mathbf{u}, \mathbf{x}) = \mathbf{f}^T\mathbf{u}. \quad (7)$$

Minimum compliance design problem can be stated by setting $f = c$ in eq. (1). Hereafter we use the mean compliance as the objective function.

Differentiating eq. (7), the following set of equations are derived

$$\frac{\partial c}{\partial x_e} = -\mathbf{u}^T\frac{\partial \mathbf{K}}{\partial x_e}\mathbf{u}, \qquad e = 1, \ldots, n. \quad (8)$$

For the term $\frac{\partial \mathbf{K}}{\partial x_e}$, based on eq. (3) and eq. (2) we can write

$$\frac{\partial \mathbf{K}}{\partial x_e} = \frac{\partial \mathbf{K}_e^g}{\partial E_e}\frac{\partial E_e}{\partial x_e} = \frac{\mathbf{K}_e^g}{E_e}\frac{\partial E_e}{\partial x_e} = \frac{\mathbf{K}_e^g}{E_e}(E^{(1)} - E^{(0)}). \quad (9)$$

Using eq. (9) in eq. (8), and noting that all the non-zero elements of $\mathbf{K}_e^g$ are related to the degrees of freedom of element e, we can write

$$\frac{\partial c}{\partial x_e} = -\frac{E^{(1)} - E^{(0)}}{E_e}\mathbf{u}_e^T\mathbf{K}_e\mathbf{u}_e, \qquad e = 1, \ldots, n, \quad (10)$$

where $\mathbf{u}_e$ is the displacement vector of element e. Substituting (10) in (6), we obtain

$$\alpha_e = \frac{E^{(1)} - E^{(0)}}{E_e}\mathbf{u}_e^T\mathbf{K}_e\mathbf{u}_e, \qquad e = 1, \ldots, n. \quad (11)$$

2.4 Switching elements and termination criterion

Different algorithms have been proposed to add and remove elements in the BESO method. Traditionally the volume constraint in eq. (1) is not satisfied in initial iterations. This will allow the BESO algorithm to start with a more relaxed version of the problem. In the algorithm introduced by Huang et al (2006) and Huang and Xie (2007) a controlling parameter called *evolutionary volume ratio* (R_v) gradually pushes the material volumes to their limits. Another parameter, called *maximum allowable admission ratio* (R_a) limits the maximum amount of materials to be added to prevent sudden changes. Once the required volume is reached, it will be kept constant by switching the same number of elements to and from each material phase. From this point froward, R_v has no effect.

In examples solved in this paper, the initial designs satisfy the volume constraint in eq. (1). The maximum allowable amount of change in each iteration is limited by a parameter called *move limit* (η) to prevent sudden

changes. This is a special case of the algorithm proposed by Huang et al (2006) with $\eta = R_a$. As noted before, R_v has no effect in this case.

To terminate the BESO procedure, the following convergence criterion can be used

$$\epsilon = \frac{|\sum_{i=1}^{s}(f_{[k-i+1]} - f_{[k-i]})|}{\sum_{i=1}^{s} f_{[k-i+1]}} \leq \tau, \tag{12}$$

where $f_{[n]}$ denotes the value of the objective function in the n-th iteration, k is the current iteration and τ is an allowable tolerance. s is a predefined number which determines the number of iterations considered in checking convergence.

In order to improve the results, in this paper a two-step termination procedure is adopted. A near convergence situation is recognized when $\tau < \epsilon \leq \tau'$. Once this criterion is satisfied, the move limit η is reduced to prevent sudden changes near convergence. Convergence is assumed when $\epsilon \leq \tau$.

In all examples solved in this paper, $s = 12$, $\tau' = 10^{-4}$, and $\tau = 10^{-6}$ are used. The move limit η is halved whenever near convergence situation is identified.

2.5 Filtering scheme for hard-kill BESO

Huang and Xie (2007) used a Filtering approach in hard-kill BESO to overcome checkerboard patterns and mesh dependency. In this approach firstly nodal sensitivities are derived by averaging sensitivities of the elements connecting to each node as follows

$$\tilde{\alpha}_j = \frac{\sum_{e\in\mathcal{E}_j} v_e \alpha_e}{\sum_{e\in\mathcal{E}_j} v_e}. \tag{13}$$

In this equation, $\mathcal{E}_j$ is the set of elements which are connected to node j and v_e denotes the volume of element e. Filtered element sensitivities are then calculated through the following filtering scheme

$$\hat{\alpha}_e = \frac{\sum_{j=1}^{N} w_{ej}\tilde{\alpha}_j}{\sum_{j=1}^{N} w_{ej}}, \tag{14}$$

where $\hat{\alpha}_e$ is the filtered sensitivity of element e, N is the number of nodes in the design domain, and w_{ej} is a weighting factor. A simple linear weighing factor can be defined as

$$w_{ej} = \max\{0, r - r_{ej}\}. \tag{15}$$

Here r is the filtering radius and r_{ej} is the distance between the centroid of element e and node j.

2.6 Using hard-kill filtering scheme in soft-kill BESO

The above BESO algorithm is used to optimize the material distribution in a short cantilever beam. The design domain, loading, supports and the initial distribution of materials are depicted in Fig. 1. The elastic moduli of the two material phases are assumed as $E^{(0)} = 0.2$ and $E^{(1)} = 1.0$. The move limit is chosen as $\eta = 6$ elements which is equivalent to 0.25% of the total number of elements in the design domain (N_D). The volume of the stronger material should not be more than 40% of the whole domain. The remaining parts of the design domain should be filled with the weaker material. The magnitude of the concentrated force is $p = 1$. Elements are all bi-linear squares with side size of $h = 1$. All units are consistent.

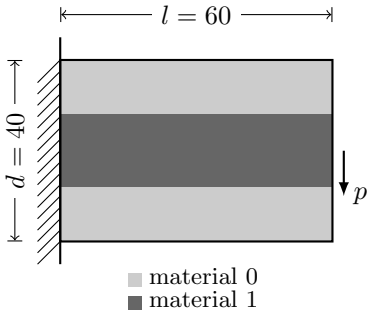

Fig. 1 Design domain and initial distribution of the two material phases in a short cantilever beam.

Fig. 2a shows the final topology obtained by applying the above BESO algorithm without using the filtering technique ($r = 0$). As expected areas with checkerboard patterns are visible in the final topology. Applying the hard-kill filtering scheme with $r = 0.05d = 2$, one obtains the topology depicted in Fig. 2b. The stiffer material phase is scattered and the topology is not recognizable.

In order to discuss the reason behind the ineffectiveness of the hard-kill filter in this example, consider a one-dimensional truss element with cross sectional area A and length L under a fixed load P. The stiffness of this element is $K = \frac{EA}{L}$ where E is the elastic modulus of the material. The sensitivity of the mean compliance with respect to changes in modulus of elasticity is

$$\frac{\partial c}{\partial E} = -\frac{1}{E} uKu = -\frac{P^2 L}{E^2 A}. \tag{16}$$

The sensitivity number $\alpha = -\frac{\partial c}{\partial E}$ is proportional to $\frac{1}{E^2}$ and increases when E decreases. In particular when $E \to 0$ we have $\alpha \to +\infty$. This is in contradiction with the hard-kill approach in which $\alpha = 0$ is assumed for $E = 0$.

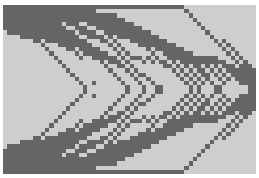

(a) $r = 0$, $c = 30.191$

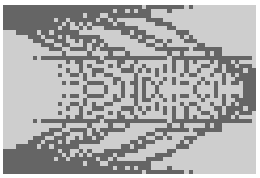

(b) $r = 2$, $c = 32.457$

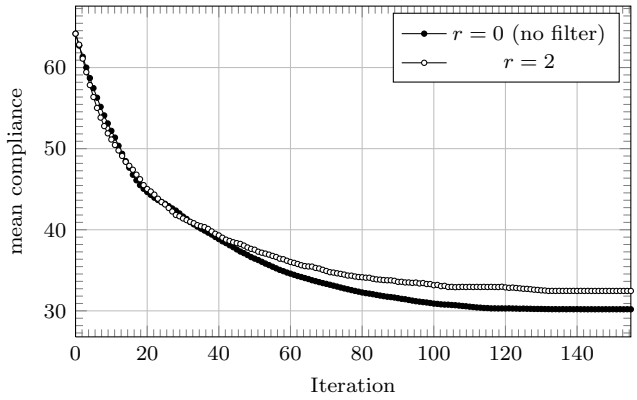

(c)

Fig. 2 Final topology obtained by applying BESO to the problem depicted in Fig. 1: a) without filtering and b) using the hard-kill filtering scheme in section 2.5. c) Evolution of objective function values for the two solutions.

The BESO routine sorts the elements based on their sensitivity numbers and switches the elements based on their ranking. Hence, what is important in BESO is the ranking of sensitivity numbers, not their numerical values. Without filtering, sensitivity numbers of different material phases will not interfere with each other and (except for checkerboard formation) the algorithm works fine. When filtering is turned on, neighboring elements will affect on each other's sensitivity number. In this case the coefficients $\frac{1}{E^{(0)}} > \frac{1}{E^{(1)}}$ in eq. (11) give more weight to soft elements in filtering. As a result, instead of the elements surrounded by stiffer material, the ones surrounded by softer material will be more likely to be switched to stiffer material and vice versa.

3 Using penalization in BESO

To tackle the deficiencies which arise in using BESO in multi-material distribution problems, Huang and Xie (2009) used a material interpolation scheme with penalization in BESO. Following the power-law interpolation scheme used in the SIMP method, Huang and Xie (2009) suggested to replace eq. (2) with

$$E_e(x_e) = E^{(0)} + x_e^p (E^{(1)} - E^{(0)}), \qquad e = 1, \ldots, n \quad (17)$$

in which $p > 1$ should be used. Using this interpolation scheme, eq. (11) changes to

$$\alpha_e = p x_e^{p-1} \frac{E^{(1)} - E^{(0)}}{E_e} \mathbf{u}_e^T \mathbf{K}_e \mathbf{u}_e, \qquad e = 1, \ldots, n. \quad (18)$$

Using $x_e = 0$ in the above equation would result in $\alpha_e = 0$. In other words, the soft-kill approach will change to hard-kill where no information is available on sensitivity of weak elements. To remedy this, Huang and Xie (2009) suggested using a very small positive value, $0 < x_{\min} \ll 1$, to represent weak elements.

In an alternative version of this approach, Ghabraie (2009) and Nguyen et al (2014) used the following alternative interpolation scheme suggested by Stolpe and Svanberg (2001)

$$E_e(x_e) = E^{(0)} + \frac{x_e (E^{(1)} - E^{(0)})}{1 + q(1 - x_e)}, \qquad e = 1, \ldots, n \quad (19)$$

in which $q > 0$ should be used. Based on this interpolation scheme, the sensitivity numbers are calculable from

$$\alpha_e = \frac{(1+q)(E^{(1)} - E^{(0)})}{[1 + q(1 - x_e)]^2 E_e} \mathbf{u}_e^T \mathbf{K}_e \mathbf{u}_e, \qquad e = 1, \ldots, n, \quad (20)$$

where $x_{\min} = 0$ can be used without causing problems.

Considering sensitivity numbers in eq. (18) and eq. (20), by increasing the penalty factors, sensitivity of weak elements reduces. In this situation, the hard-kill filtering scheme in section 2.5 can work effectively if sufficiently large penalty factors are applied.

Fig. 3 shows the solutions to the previous problem using the interpolation scheme in eq. (17) assuming $x_{\min} = 0.001$ with $p = 1.2$, $p = 1.3$, and $p = 1.5$. It can be seen that the checkerboard patterns are eliminated and the final topologies are clear.

In this example, penalty factor values smaller than 1.2 did not completely eliminate the numerical anomalies. For values $1.2 < p < 1.5$ the final topology and final value of the objective function depended on the penalty factor, as illustrated in Fig. 3. For $p \geq 1.5$ the solution did not change by further increasing the penalty factor.

Although by using a sufficiently large penalty factor this approach can solve the deficiencies visible in Fig. 2, using penalization in BESO where no intermediate density is present does not have any physical meaning. Moreover, final topologies obtained in this approach can depend on the penalty factor as illustrated in Fig. 3.

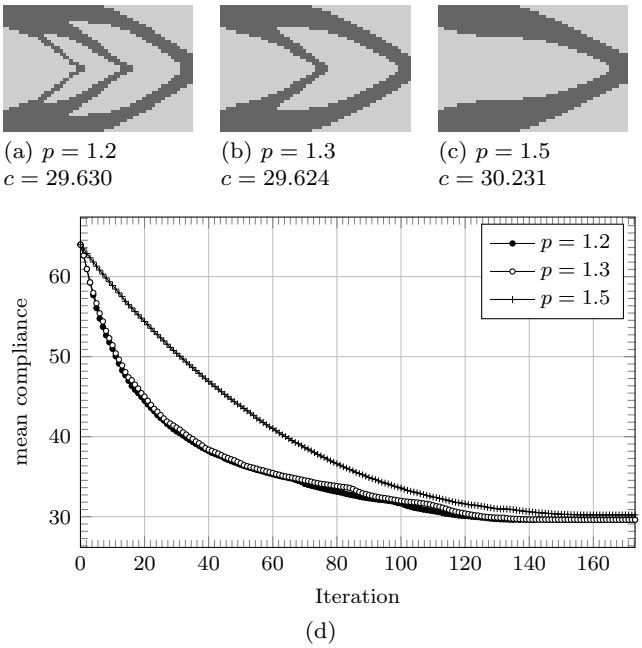

Fig. 3 Final topology obtained by BESO using different penalty factors: a) $p = 1.2$, b) $p = 1.3$, and c) $p = 1.5$. d) Eevolution of objective function values.

4 Alternative filtering scheme

Instead of using penalization, a different filtering scheme is proposed here to eliminate the numerical anomalies demonstrated in section 2.6. In the new filtering scheme, eq. (13) is replaced by the following equation

$$\tilde{\alpha}_j = \frac{\sum_{e\in\mathcal{E}_j} v_e E_e \alpha_e}{\sum_{e\in\mathcal{E}_j} v_e E_e}. \tag{21}$$

By multiplying element sensitivities by their elastic moduli, this scheme cancels the effect of the coefficient $\frac{1}{E_e}$ in eq. (11).

The final topology obtained for the short cantilever beam using this filter and the linear interpolation scheme is illustrated in Fig. 4. The proposed approach successfully eliminated all checkerboard patterns. Because this filtering scheme works well with linear interpolation scheme, it also eliminates the need for introducing the concept of penalization in BESO.

5 Gradual BESO (*g*BESO)

Continuation approaches are used in combination with methods like SIMP to overcome the local minima problem. In these approaches, a near convex version of the problem is solved first and the problem is gradually changed in steps towards the original problem after the previous step is converged. For example, one can start

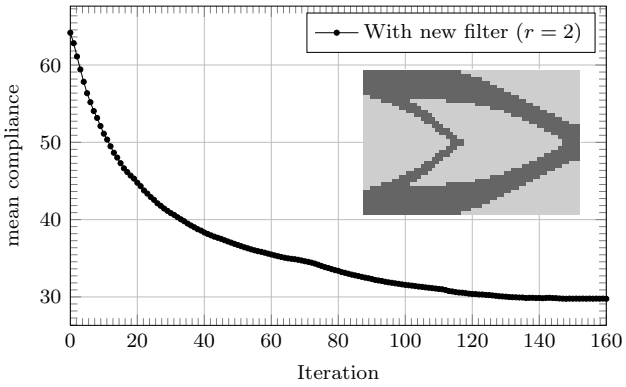

Fig. 4 Final topology obtained by applying the new filtering scheme and evolution of objective function values. The final value of the objective function is $c = 29.760$.

the problem with a penalty factor close to unity and then gradually increase the penalty factor to eliminate intermediate densities.

A similar concept is used here to propose a further improvement to the soft-kill BESO method. In this approach the problem is solved in a number of *steps*. A near convex sub-problem is initially considered in the first step with all material phases having elastic moduli values very close to the softest material. After solving the sub-problem in each step, the algorithm proceeds to the next step where the elastic moduli of the stiffer materials are gradually increased. This procedure is repeated until the elastic moduli of all material phases reach their required values. For two material phases, such procedure can be expressed as follows

$$\begin{aligned} E^{(1)}_{\langle 1\rangle} &= G_0 E^{(0)}, \\ E^{(1)}_{\langle s\rangle} &= G_1 E^{(1)}_{\langle s-1\rangle}, \quad s > 1, \end{aligned} \tag{22}$$

where $E_{\langle s\rangle}$ denotes the value of E at step s, and $G_0 > 1$ and $G_1 > 1$ are two predefined factors. The G_0 factor should be chosen close to 1 to ensure that the initial sub-problem is near convex.

To explain the rationale behind the proposed gradual approach, consider the following two-material compliance minimization problem which is a special case of eq. (1),

$$\begin{aligned} \min_{\mathbf{x}\in\mathcal{X}^n} \quad & c(\mathbf{x}) \\ \text{such that} \quad & V_1(\mathbf{x}) \le \bar{V}_1. \end{aligned} \tag{23}$$

BESO solves a discrete version of this problem with $\mathcal{X} = \{0, 1\}$. The continuous version of this problem, i.e. when $\mathcal{X} = [0, 1]$ is equivalent to the variable thickness sheet problem and is convex.

As shown by Ghabraie (2014), the changes in mean compliance due to changing the design variable of ele-

ment e can be expressed as

$$\underset{e}{\Delta c} = \sum_{m=1}^{\infty} \frac{1}{m!} \frac{\partial^m c}{\partial {x_e}^m} \Delta {x_e}^m = \sum_{m=1}^{\infty} \mathbf{u}^T \frac{\partial \mathbf{K}}{\partial x_e} \left(\mathbf{K}^{-1} \frac{\partial \mathbf{K}}{\partial x_e} \right)^{m-1} \mathbf{u} \, \Delta {x_e}^m. \quad (24)$$

Using eq. (9) in this equation we obtain

$$\underset{e}{\Delta c} = \sum_{m=1}^{\infty} \mathbf{u}^T \mathbf{K}_e^g \left(\mathbf{K}^{-1} \mathbf{K}_e^g \right)^{m-1} \mathbf{u} \left(\frac{\Delta E}{E_e} \Delta x_e \right)^m, \quad (25)$$

where $\Delta E = E^{(1)} - E^{(0)}$. We have

$$\frac{\Delta E}{E_e} = \begin{cases} \frac{E^{(1)}}{E^{(0)}} - 1, & \text{if } E_e = E^{(0)}, \\ 1 - \frac{E^{(0)}}{E^{(1)}}, & \text{if } E_e = E^{(1)}. \end{cases} \quad (26)$$

Hence,

$$\lim_{\frac{E^{(1)}}{E^{(0)}} \to 1} \left| \frac{\Delta E}{E_e} \right| = 0. \quad (27)$$

So if the ratio $\frac{E^{(1)}}{E^{(0)}}$ approaches one, we can ignore the higher order terms in eq. (25) and write

$$\frac{\underset{e}{\Delta c}}{\Delta x_e} = \mathbf{u}^T \mathbf{K}_e^g \mathbf{u} \frac{\Delta E}{E_e} = \mathbf{u}_e^T \mathbf{K}_e \mathbf{u}_e \frac{\Delta E}{E_e} = \alpha_e. \quad (28)$$

In this case, the sensitivity numbers used in BESO approach the sensitivities of the continuous problem. In other words, the discrete problem solved by BESO method approaches the continuous variable thickness sheet problem[1]. In gradual BESO, G_0 defines the ratio $\frac{E^{(1)}}{E^{(0)}}$ for the initial sub-problem and thus need to be selected close to one to make the initial sub-problem near convex. Effects of the gradual parameters on final results are studied in section 7.

To demonstrate the application of gBESO , the previous short cantilever beam problem is solved with gradual BESO setting $G_0 = 1.0001$ and $G_1 = 1.25$. This means that the procedure starts with $E_{\langle 1 \rangle}^{(0)} = 0.2$ and $E_{\langle 1 \rangle}^{(1)} = 1.0001 \times E^{(0)} = 0.20002$ in the first step, and after convergence of each step $E^{(1)}$ is increased by 25% until it reaches the target value of 1. The results obtained by this procedure are illustrated in Fig. 5 and Fig. 6.

Fig. 5 shows the evolution of mean compliance values in this example. The solid line shows the values of the mean compliance at each step calculated based on the elastic moduli of materials at that step, i.e. $E_{\langle s \rangle}^{(1)}$ is used to calculate the mean compliance at step s. These values are listed above the graph. Because the stiffness of the stiffer material phase is increasing throughout the solution, significant drops are visible when the algorithm proceeds to the next step.

After obtaining displacements by finite element analysis, if mean compliance is calculated based on the target elastic moduli of material phases (here $E^{(1)} = 1$),

[1] Another conclusion is that the results of the variable thickness sheet problem will have less elements with intermediate thickness (grey elements) when the maximum and minimum allowed thicknesses are chosen close to each other. See Table 1.

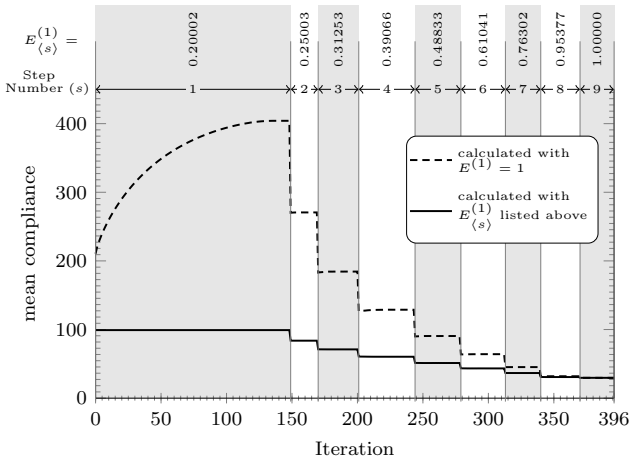

Fig. 5 Evolution history of mean compliance values obtained by applying the gradual BESO method to the problem depicted in Fig. 1.

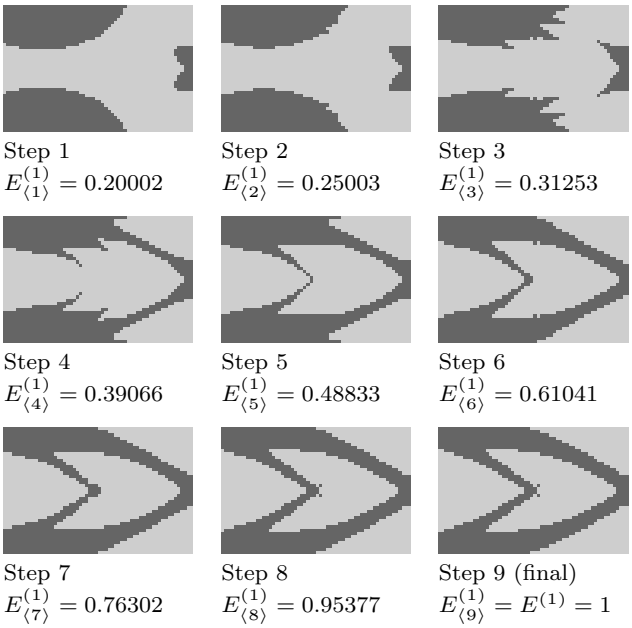

Fig. 6 Topologies obtained at the end of each step of the gradual BESO procedure. Values of elastic modulus of the stiffer material phase in each step is noted below each figure. Elastic modulus of the softer material phase is $E^{(0)} = 0.2$ in all steps.

the dashed line is obtained. Convergence of each step is determined based on these values.

Topologies at the end of each step (solutions to the sub-problems) are shown in Fig. 6. In this figure, the lighter shades depict the weak material with $E^{(0)} = 0.2$ while the darker shades show the stiffer material. The value of the elastic modulus of the stiffer material is noted under the final topology of each step. The final solution is obtained at the end of the 9th step where elastic modulus of the stiffer material reached the target value of $E^{(1)} = 1$. In this example the final topology is very similar to the one depicted in Fig. 4 which was obtained without using the gradual stiffening procedure. The final value of the objective function is slightly improved by using the gradual procedure and reduced from 29.760 to 29.623.

In following sections further examples are solved to illustrate the capabilities of the proposed approach and its superiority over the normal BESO algorithm.

6 Further examples

6.1 Simply supported beam

A simply supported beam is considered as another example with the design domain, loading, and supports illustrated in Fig. 7. A mesh of 120×40 bilinear square elements are used to model half of the design domain making use of symmetry. The total volume of the design domain is to be equally shared between two materials. These two materials are considered to have the elastic moduli of $E^{(1)} = 1$ GPa and $E^{(0)} = 0.1$ GPa. A filtering radius of $r = 3$ mm is used to make this example comparable to the one solved by Huang and Xie (2009).

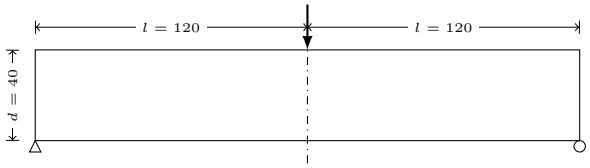

Fig. 7 Design domain of a simply supported beam. All dimensions are in mm.

The values of $G_0 = G_1 = 2$ and $\eta = 0.005N_D = 24$ elements are adopted in this example. The initial material distribution and the final topology obtained is shown in Fig. 8 with the final objective function value of 4.173 N · mm. This solution is not significantly different from the one reported by Huang and Xie (2009) but provides a slightly smaller value of the objective function.

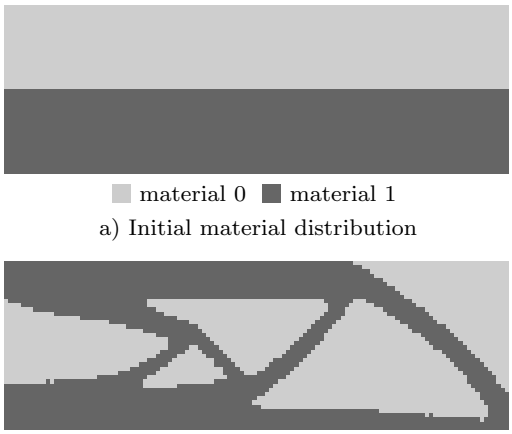

a) Initial material distribution

b) $c = 4.173$ N · mm

Fig. 8 A simply supported beam optimized using the gradual BESO approach: a) initial material distribution, and b) the obtained topology. The two materials have the elastic moduli of $E^{(1)} = 1$ GPa and $E^{(0)} = 0.1$ GPa.

6.2 Starting from different initial designs

Using the proposed gradual BESO, if G_0 is sufficiently close to 1, it is possible to obtain the same solution from different initial designs. To numerically illustrate this, four different initial designs are selected for the short cantilever beam problem. Results obtained with and without applying the gradual procedure are illustrated in Fig. 9. In this example, a mesh size of 120×80 with a small filtering radius of $r = 0.025d$ is used (d is the depth of the design domain as shown in Fig. 1). Using smaller filtering radius makes the problem more susceptible to local minima. The move limit is chosen as $\eta = 0.0021N_D = 20$ elements and gradual parameters are similar to the example solved in section 5.

It can be seen that without the gradual procedure, final topologies depend on initial designs. However, by using the proposed gradual procedure, identical final results are obtained for all four initial designs.

The proposed approach is also useful in single material distribution problems. In this case the voids can be modeled by a very soft material with an elastic modulus value significantly smaller than that of the base material. Here, the previous example is solved again with material properties of $E^{(1)} = 1$ and $E^{(0)} = 10^{-4}$ representing voids. $G_0 = 1.0001$ is adopted again but G_1 is increased to 5 to speed up the solution procedure. All other parameters are similar to the previous example. The results are reported in Fig. 10.

Without using the gradual procedure, final topologies vary significantly for different initial designs. Using gradual BESO results in identical topologies. These results show that using appropriate parameters, the pro-

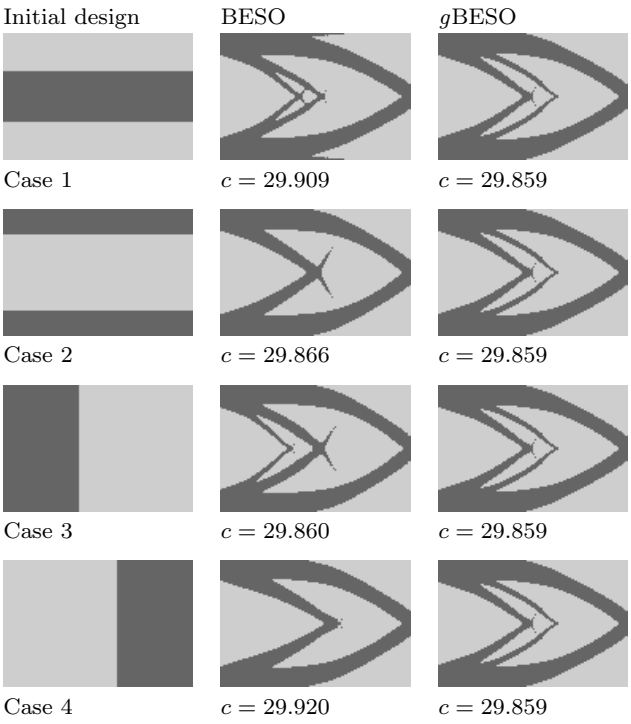

Fig. 9 The proposed gradual approach is used to obtain similar solution starting from different initial designs in a two-phase material distribution problem.

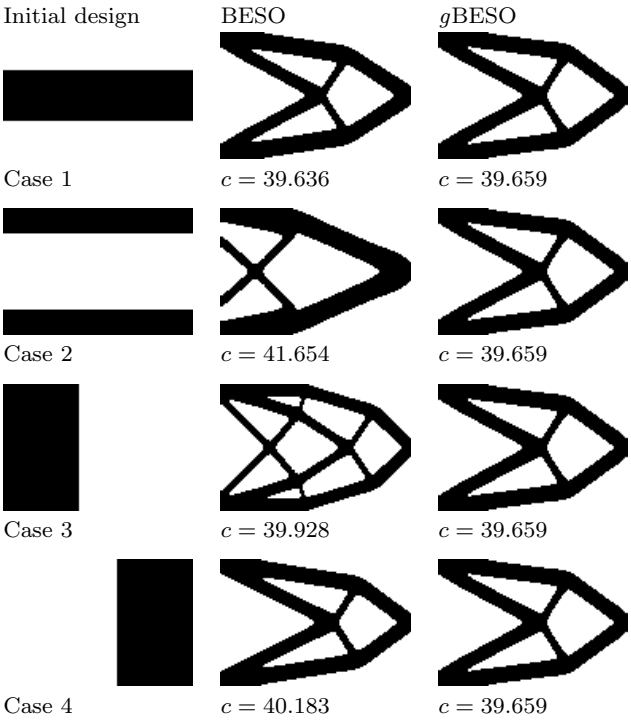

Fig. 10 The proposed gradual approach is used to obtain similar solution starting from different initial designs in a single material distribution problem.

posed gradual BESO is not sensitive to the initial design in single or in multiple material distribution problems.

For comparison and verification, the same problem is solved using SIMP method with $p = 3$, with and without using continuation approach. In order to let the SIMP method handle these problems, in the initial designs, the voids are represented by $x = 0.001$ instead of $x = 0$. The continuation approach starts with a large filtering radius of $r_0 = 0.25d$ and after convergence of each step the filtering radius is halved. A similar termination criterion is employed in the SIMP method to make a valid comparison. Fig. 11 shows the obtained topologies and final values of the objective function in each case.

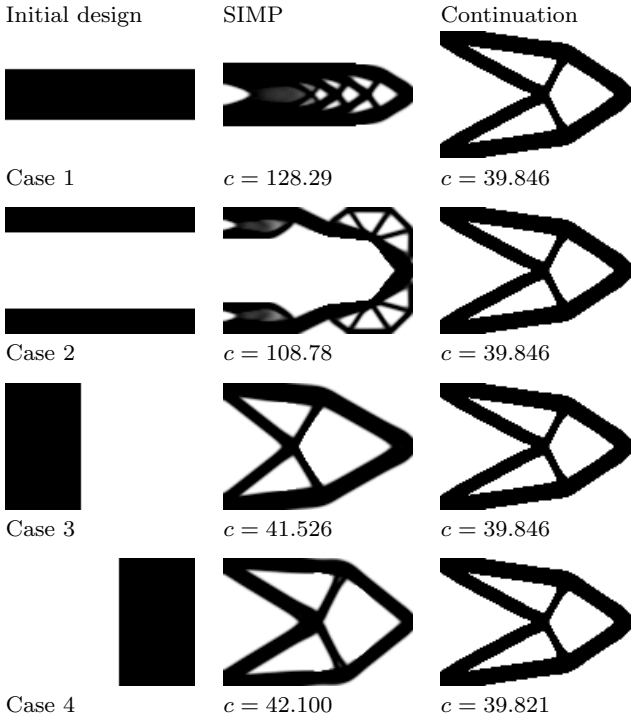

Fig. 11 The solutions obtained using the SIMP method with and without the continuation approach for different initial designs. In all cases penalty factor of $p = 3$ is used.

As expected the SIMP method, like the normal BESO method, is prone to the local minima problem. Using the continuation approach rectifies this problem. The solutions obtained via the continuation approach match well with the result of gradual BESO.

6.3 Sensing unused supports

In problems with a void phase (or an extremely soft material compared to other materials), if a support (or

a separated solid area) is surrounded by a large area of void elements, the normal BESO method may not be able to "sense" that support (or solid area). This behavior was first demonstrated by Zhou and Rozvany (2001). The proposed gradual BESO algorithm can fix this deficiency. To demonstrate this a simple example with the initial design illustrated in Fig. 12 is considered. The design domain is discretized using a mesh of 100×100 bilinear square elements. 25% of this domain is to be filled with a material with elastic modulus of $E^{(1)} = 1$ while the voids are modeled using $E^{(0)} = 10^{-4}$. A filtering radius of $r = 5h$ is used where $h = 1$ is the size of the elements. The units are all consistent. The results obtained with and without using the gradual procedure are reported in Fig. 12. Here a move limit of $\eta = 0.001N_D = 10$ elements is used and the gradual parameters are selected as $G_0 = 1.01$ and $G_1 = 2$.

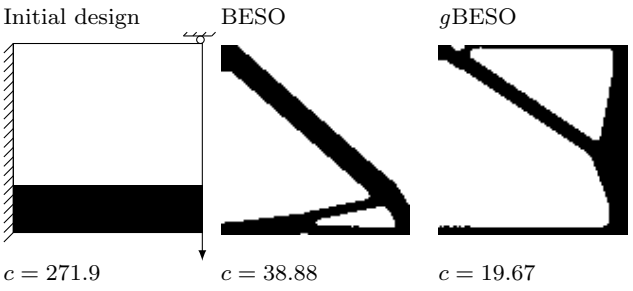

Fig. 12 A simple example showing the superiority of the proposed gradual BESO over normal BESO ($\eta = 10$, $G_0 = 1.01$, and $G_1 = 2$).

It can be seen that without using the gradual procedure the algorithm is not capable of making use of the roller support resulting in a solution with $c = 38.88$. Using the gradual BESO procedure, the final value of the objective function is reduced by about 98% to $c = 19.67$.

6.4 More than two material phases

The approach proposed for two materials can be easily extended to problems with more material phases. The linear interpolation scheme can be extended to the following form

$$E_e(x_e) = E^{(i-1)} + (x_e - i + 1)(E^{(i)} - E^{(i-1)}), \quad \text{for} \quad i-1 \le x_e \le i, \; i = 1, \dots, m-1, \; e = 1, \dots, n \tag{29}$$

which maps E_e to $E^{(0)}, E^{(1)}, \dots, E^{(m-1)}$ respectively for $x_e = 0, 1, \dots, m-1$. Based on this interpolation scheme, sensitivity numbers for the compliance minimization problem take the form

$$\alpha_e = \frac{E^{(i)} - E^{(i-1)}}{E_e} \mathbf{u}_e^T \mathbf{K}_e \mathbf{u}_e, \quad \text{for} \quad i-1 \le x_e \le i, \; i = 1, \dots, m-1, \; e = 1, \dots, n. \tag{30}$$

In each iteration, the switching procedure will be completed in an internal loop over the material phases. In iteration i ($i = 1, \dots, m-1$) of this internal loop, elements are only switched between material phases i and $i-1$. Before switching, sensitivity numbers will be filtered using the new filtering scheme introduced in section 4.

This approach is tried on the short cantilever beam with three material phases. The three phases have the elastic moduli of $E^{(0)} = 0.2$, $E^{(1)} = 0.5$, and $E^{(2)} = 1$. The maximum allowable volume for material phases are $\bar{V}_1 = \bar{V}_2 = 0.2V_T$ where V_T is the total volume of the design domain. The initial design is shown in Fig. 13. A 120×80 mesh is used with the filtering radius of $r = 2h$ where h is the size of elements. The move limit for switching between any pair of material phases is selected as $\eta = 10$ elements equivalent to 0.1% of the total number of elements in the design domain.

In order to check the evolution of the objective function values, the problem is initially solved without using the gradual procedure. The results are illustrated in Fig. 13. As shown in this figure, the mean compliance monotonically decreases and converges at $c = 40.142$.

The problem is also solved using the proposed gradual BESO. To apply the gradual stiffening procedure in multi-phase material problems, the highest elastic modulus $E^{(m-1)}$ is taken as the reference and step values of elastic moduli of other material phases are interpolated at each step. Hence, eq. (22) is expanded to the following

$$\begin{aligned} E_{\langle 1 \rangle}^{(m-1)} &= G_0 E^{(0)}, \\ E_{\langle s \rangle}^{(m-1)} &= G_1 E_{\langle s-1 \rangle}^{(m-1)}, \quad s > 1, \\ E_{\langle s \rangle}^{(i)} &= E^{(0)} + \frac{E_{\langle s \rangle}^{(m-1)} - E^{(0)}}{E^{(m-1)} - E^{(0)}} \times (E^{(i)} - E^{(0)}), \\ & \qquad i = 1, \dots, m-2. \end{aligned} \tag{31}$$

In this example, $G_0 = 1.0001$ and $G_1 = 1.5$ are adopted. The final topology obtained via gradual BESO is shown in Fig. 13. The final value of the mean compliance in this case is $c = 40.063$ which shows a slight

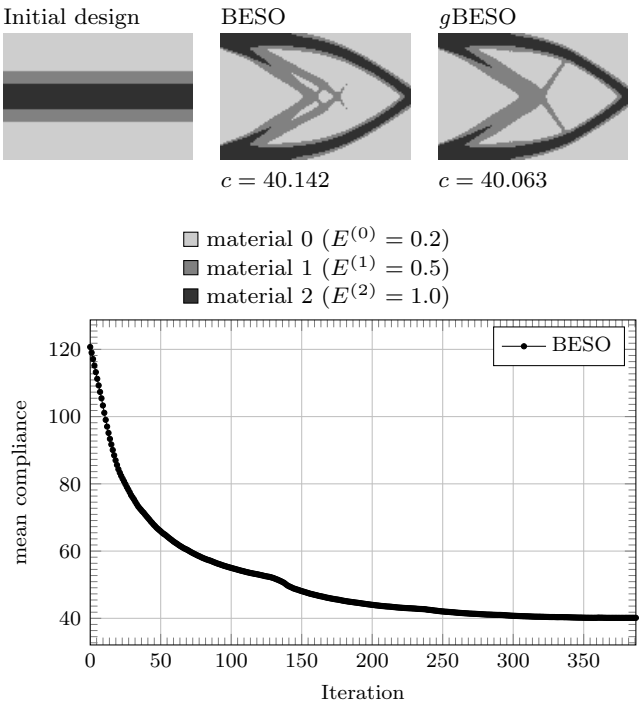

Fig. 13 Solving a short cantilever beam problem with three material phases.

improvement compared to the solution obtained without using the gradual approach.

To further demonstrate the capabilities of the proposed approach in handling multiple material phases, the short cantilever beam problem is solved with five material phases. The initial design is shown in Fig. 14. The elastic moduli of the five phases are assumed to be $E^{(0)} = 10^{-4}$, $E^{(1)} = 10^{-3}$, $E^{(2)} = 10^{-2}$, $E^{(3)} = 10^{-1}$, and $E^{(4)} = 1$. All material phases should occupy 20% of the design domain.

Gradual BESO is used with $G_0 = 1.0001$ and $G_1 = 5$. Other parameters are the same as the previous 3-material problem. The final value of the mean compliance is $c = 67.368$. The initial design and step topologies are depicted in Fig. 14.

Three other initial designs are also considered for this short cantilever beam. As shown in Fig. 15, gradual BESO yields the exact same result for all these initial designs.

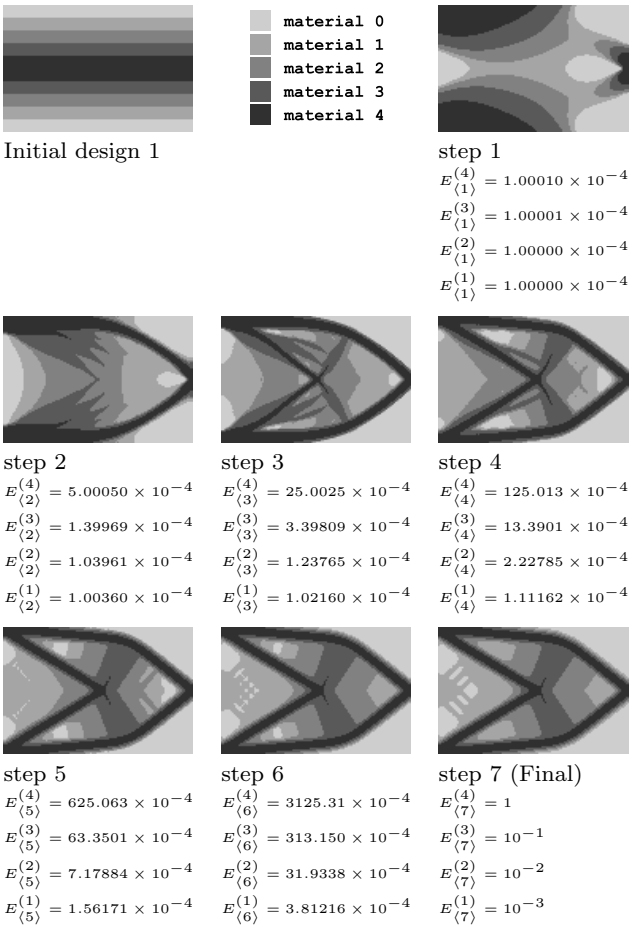

Fig. 14 Initial design and step topologies obtained by using gradual BESO on a 5-material design problem. In all steps $E^{(0)} = 10^{-4}$.

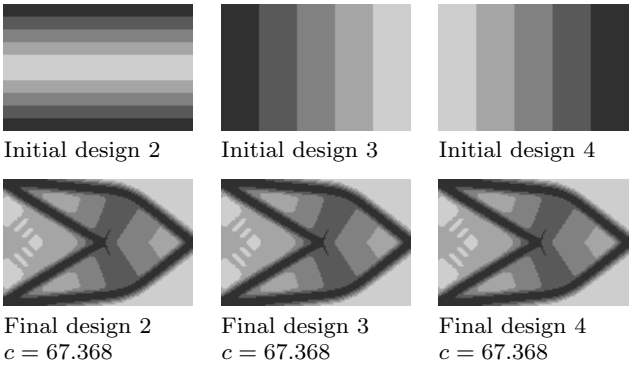

Fig. 15 Final topologies obtained by using gradual BESO on a 5-material design problem with different initial disigns.

6.5 More than one material phases and voids

Considering a very soft material to represent voids, the proposed method can be used to solve problems in which more than one material phases are to be distributed among voids in the design domain. The first example considered is the simply supported beam shown in Fig. 7. Two materials with $E^{(2)} = 1$ GPa and $E^{(1)} =$

0.1 GPa are to be used to fill 15% and 25% of the design domain volume respectively. The rest 60% of the design domain should be filled with a very soft material with $E^{(0)} = 10$ kPa representing voids. Filtering radius is $r = 3$ mm. All algorithmic parameters are selected similar to the example shown in Fig. 8 ($\eta = 0.005N_D = 24$ elements, $G_0 = G_1 = 2$).

The initial design and the final solution obtained using the gradual BESO procedure are illustrated in Fig. 16. The obtained topology is simpler and the objective function is almost 7% lower than the one reported by Huang and Xie (2009) for the same problem ($c = 13.0$ N.mm).

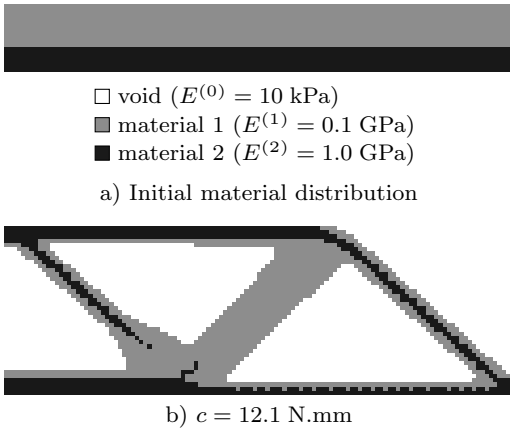

Fig. 16 A simply supported beam of Fig. 7 is solved with two materials and voids: a) the initial material distribution, and b) the results obtained using the gradual BESO approach.

Another simply supported structure is considered with the design domain depicted in Fig. 17. The dimensions are $l = 6$ m and $P = 15$ kN. Due to symmetry only half of the domain is modeled using a 240×240 mesh. Two examples are solved on this design domain, one with two materials and voids and the other one with three materials and voids. The adopted parameters in both examples are $r = 0.1$ m, $\eta = 120$, $G_0 = 1.05$ and $G_1 = 10$.

In the first of these examples, two materials with $E^{(1)} = 100$ GPa and $E^{(2)} = 200$ GPA are distributed in the design domain filling 20% and 10% of its volume respectively. The rest 70% is occupied by a very soft material with $E^{(0)} = 100$ kPa representing voids. The initial design and the obtained solution are shown in Fig. 18.

In the three material design, like the two material one the voids are represented by $E^{(0)} = 100$ kPa. The

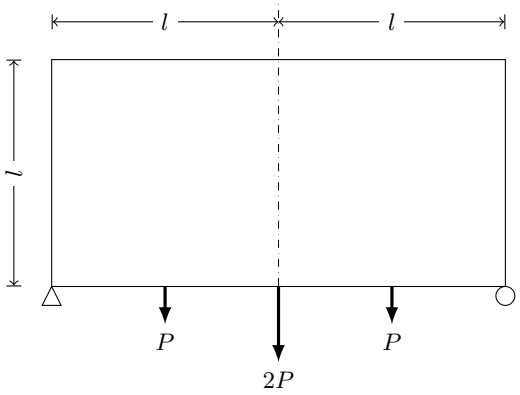

Fig. 17 Design domain, loads and supports for a simply supported Michell-type structure.

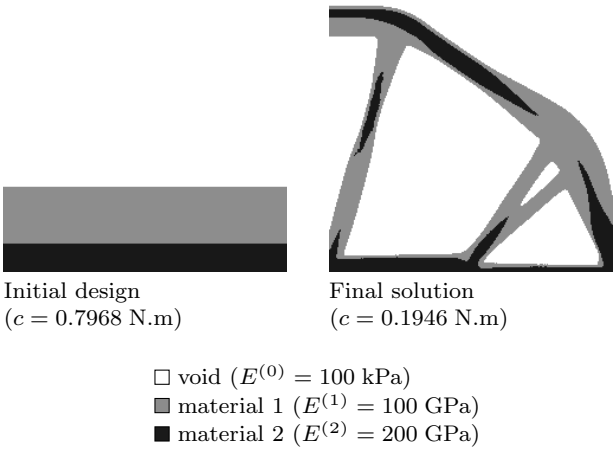

Fig. 18 The initial design and the final solution obtained for the Michell-like structure (Fig. 17) with two materials and voids.

three material phases have $E^{(1)} = 50$ GPa, $E^{(2)} = 100$ GPA and $E^{(3)} = 200$ GPA all of which limited to filling 10% of the design domain. The initial design and the obtained solution are shown in Fig. 19. The results shown in Fig. 18 and Fig. 19 are comparable with solutions provided by Wang and Wang (2004).

7 The effects of gradual parameters

In this section we study the effects of the move limit η and the gradual parameters G_0 and G_1 on the performance of the proposed gBESO approach. The problem depicted in Fig. 12 is considered in this part due to its particular nature.

The move limit (η) defines the maximum number of elements which can be switched in each iteration. One would generally expect that the lower the move limit, the better the solution. Results obtained for various values of the move limit are shown in Fig. 20. The gradual

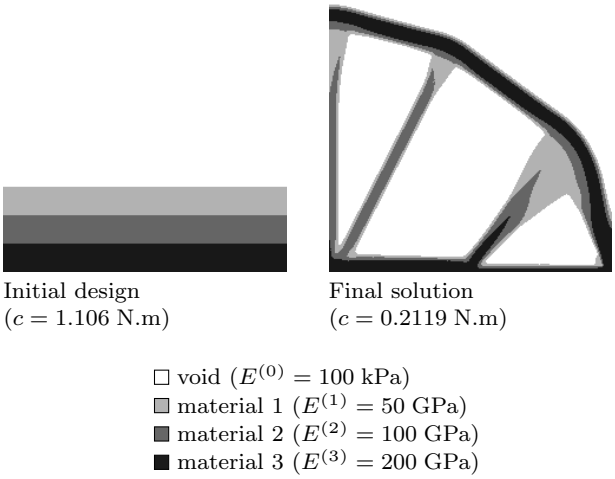

Fig. 19 The initial design and the final solution obtained for the Michell-like structure (Fig. 17) with three materials and voids.

parameters are $G_0 = 1.01$ and $G_1 = 2$. As expected increasing the move limit increases the final value of the objective function.

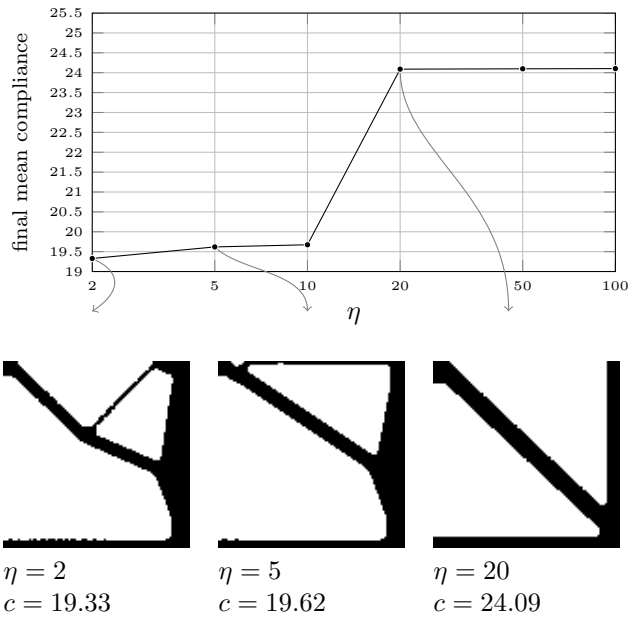

Fig. 20 The effect of changing move limit (η) on final solutions of the problem shown in Fig. 12.

The gradual parameter G_1 defines how fast the materials' elastic moduli would approach their final values. In other words, the number of steps required to complete the gradual procedure can be controlled by G_1. Choosing smaller values for G_1 can result in more iterations but it causes smoother transition between the sub-problems and hence better solutions are generally expected.

To study the effect of G_1 on final solutions, the move limit is fixed at $\eta = 10$ and $G_0 = 1.01$ is chosen. The problem is solved with different values of G_1. Fig. 21 summarizes the results. Although some random oscillation are observable, as expected, increasing G_1 can significantly increase the final value of the objective function.

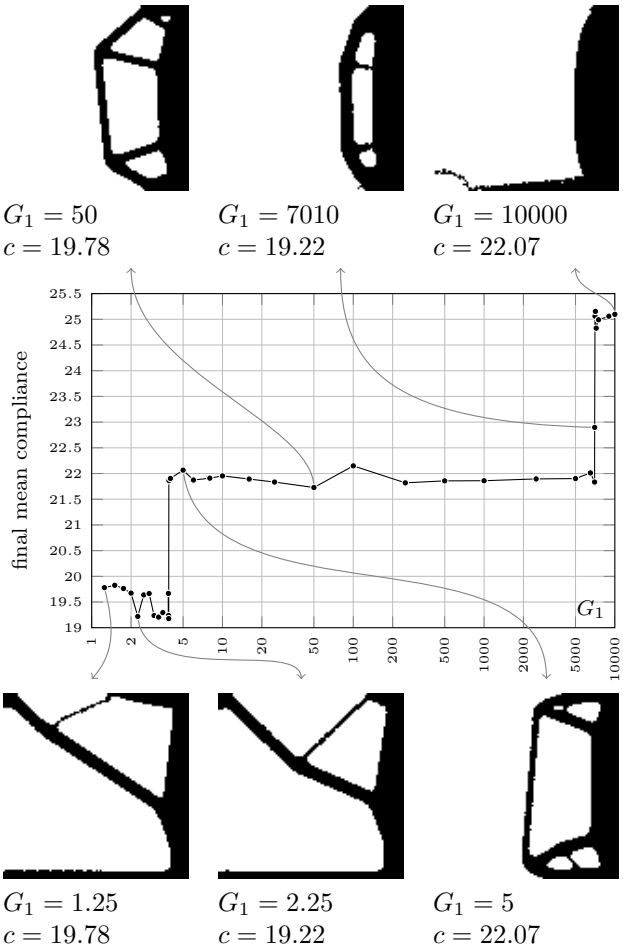

Fig. 21 Final values of the objective function (mean compliance) for the problem shown in Fig. 12 with $\eta = 10$, $G_0 = 1.01$ and different G_1 values.

A number of different final topologies obtained in this test are depicted in Fig. 21. It is interesting to note the big jumps around $G_1 = 4$ and $G_1 = 7000$. The solutions with $G_1 < 4$ effectively used both supports. With $4 \leq G_1 \leq 7000$ only the roller support at top right corner of the design domain (see Fig. 12) is used. Looking at the solution of the first sub-problem (Fig. 22d) and comparing it to the topologies shown in Fig. 21, one can see that for large values of G_1, it seems

that the final solutions were trapped in the local minima close to Fig. 22d. The small number of steps and big jumps between the material properties used in the sub-problems prevent the algorithm from finding better solutions.

Another interesting point to note is that despite the variety, all the solutions in Fig. 21 are better than the normal BESO solution for this problem (see Fig. 12). This is due to the suitable G_0 value which is chosen close to one in this case.

Regarding the gradual parameter G_0, as explained before, this value should be chosen close to one to make the initial sub-problem near convex. In section 5, it was mentioned that for G_0 values close to one, the solution of the first gBESO sub-problem would be close to the continuous version of the same problem (variable thickness sheet). This is demonstrated in Fig. 22 and Table 1.

Table 1 Comparing the results of the BESO (binary) and variable thickness sheet (continuous) versions of the optimization problem (eq. 23) for different values of $\frac{E^{(1)}}{E^{(0)}}$ ($E^{(0)} = 10^{-4}$). The design domain and the initial design are shown in Fig. 12.

$\frac{E^{(1)}}{E^{(0)}}$	final c value		diff. (%)	Percentage of grey elements in vts solutions
	variable thickness sheet (vts)	BESO		
1.01	138476	138477	0.001	0.68
2	75807	75929	0.16	14.3
5	33041	33961	2.79	28.6
10	17251	18074	4.77	41.2
20	8867	9621	8.50	52.0
50	3619	4221	16.6	66.0

It can be seen in Fig. 22 and Table 1 that BESO solutions are similar to those of variable thickness sheet problem when $\frac{E^{(1)}}{E^{(0)}}$ is close to one. As this ratio grows solutions of the two problem deviate from each other. Hence, if G_0 value is not chosen small enough, the gBESO procedure might not be effective.

To further study the effect of G_0 value on final solutions, different G_0 values are tested with $\eta = 10$ and $G_1 = 2$. The results are summarized in Fig. 23. It can be seen that lower values of G_0 are advisable to ensure better solutions. Although in this case $15 \leq G_0 \leq 18$ also resulted in good solutions for this problem, there is no guarantee that this behavior happens with other problems. For $G_0 = 10000$, we have $E^{(1)}_{\langle 1 \rangle} = E^{(1)}$ and the gradual BESO will behave exactly like normal BESO.

It should be noted that although in all the examples shown here, the proposed gradual BESO yields better solution than normal BESO, this is not necessarily always the case. If one starts a problem with an initial design very close to the optimal solution, it is possible

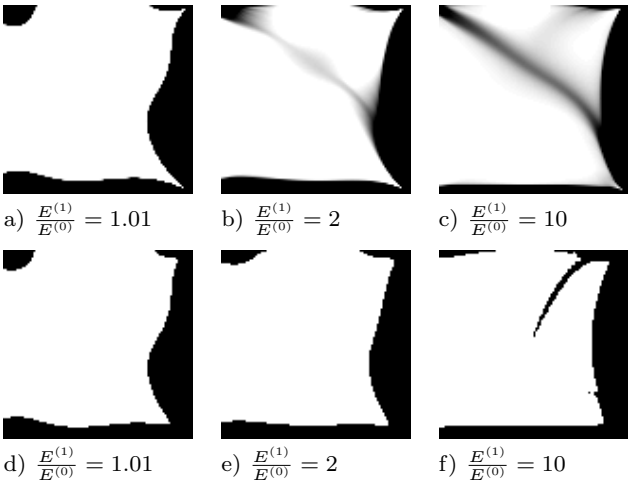

Fig. 22 Comparing the final solutions of continuous (a-c) and binary (d-f) versions of the optimization problem (eq. 23) for different ratios of $\frac{E^{(1)}}{E^{(0)}}$ ($E^{(0)} = 10^{-4}$). The design domain and the initial design are shown in Fig. 12.

that normal BESO converges to a better solution than gradual BESO, because the latter will possibly move away from the initial design when solving its first sub-problem. However, in general it is expected that gradual BESO converges to better solutions in compare to normal BESO as demonstrated in this paper.

8 Conclusion

The soft-kill BESO method has been improved and applied to single and multi-phase material distribution problems. Instead of using a penalty factor, a new filtering scheme is proposed for the soft-kill BESO method to eliminate numerical anomalies which arise in multiple material distribution problems. A continuation approach by gradual stiffening of materials is also introduced to improve the results of soft-kill BESO. The algorithm is extended to any number of material phases.

Capabilities of the proposed approach are tested through a number of examples. It is demonstrated that the proposed gradual BESO approach is capable of handling problems with several material phases and is not sensitive to initial designs. It is also illustrated that unlike the traditional hard-kill BESO method, the proposed method is capable of making use of redundant supports and recovering broken links.

References

Bendsøe MP (1989) Optimal shape design as a material distribution problem. Structural Optimization 1(4):193–202, DOI 10.1007/BF01650949

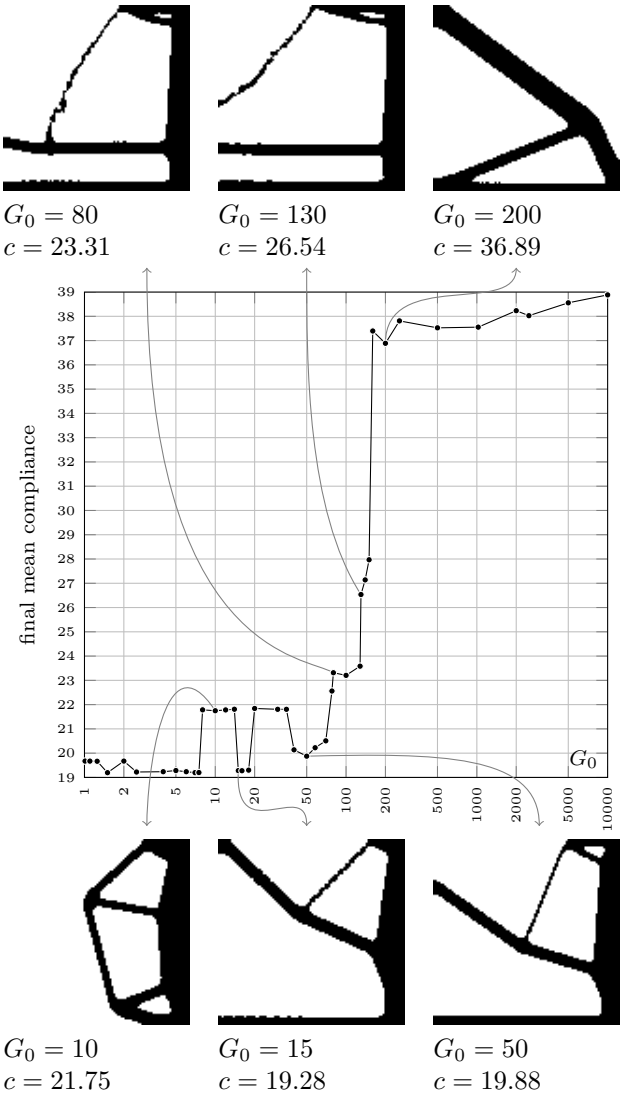

Fig. 23 Final objective function values (mean compliance) for the problem shown in Fig. 12 with $\eta = 10$, $G_1 = 2$ and different G_0 values.

Bendsøe MP, Kikuchi N (1988) Generating optimal topologies in structural design using a homogenization method. Computer Methods in Applied Mechanics and Engineering 71(2):197–224, DOI 10.1016/0045-7825(88)90086-2

Bendsøe MP, Sigmund O (1999) Material interpolation schemes in topology optimization. Archive of Applied Mechanics 69(9-10):635–654, DOI 10.1007/s004190050248

Blasques JP, Stolpe M (2012) Multi-material topology optimization of laminated composite beam cross sections. Composite Structures 94(11):3278–3289, DOI 10.1016/j.compstruct.2012.05.002

Bruyneel M (2011) SFP—a new parameterization based on shape functions for optimal material selection: application to conventional composite plies. Structural and Multidisciplinary Optimization 43(1):17–27, DOI 10.1007/s00158-010-0548-0

Deaton JD, Grandhi RV (2014) A survey of structural and multidisciplinary continuum topology optimization: post 2000. Structural and Multidisciplinary Optimization 49(1):1–38, DOI 10.1007/s00158-013-0956-z

Gao T, Zhang W (2011) A mass constraint formulation for structural topology optimization with multiphase materials. International Journal for Numerical Methods in Engineering 88(8):774–796, DOI 10.1002/nme.3197

Gao T, Zhang W, Duysinx P (2013) Simultaneous design of structural layout and discrete fiber orientation using bi-value coding parameterization and volume constraint. Structural and Multidisciplinary Optimization 48(6):1075–1088, DOI 10.1007/s00158-013-0948-z

Ghabraie K (2009) Exploring topology and shape optimisation techniques in underground excavations. PhD thesis, School of Civil, Environmental and Chemical Engineering Science, RMIT University, Melbourne, Australia

Ghabraie K (2014) The ESO method revisited. Structural and Multidisciplinary Optimization pp 1–12, DOI 10.1007/s00158-014-1208-6

Ghabraie K, Xie YM, Huang X (2010a) Using BESO method to optimize the shape and reinforcement of underground openings. In: Ghafoori N (ed) Challenges, Opportunities and Solutions in Structural Engineering and Construction: Proceedings of the 5th International Structural Engineering and ConstructiomConference (ISEC-5), 22-25 Sep. 2009, Las Vegas, USA, Taylor and Francis, London, pp 1001–1006

Ghabraie K, Xie YM, Huang X, Ren G (2010b) Shape and reinforcement optimization of underground tunnels. Journal of Computational Science and Technology 4(1):51–63, DOI 10.1299/jcst.4.51

Huang X, Xie YM (2007) Convergent and mesh-independent solutions for the bi-directional evolutionary structural optimization method. Finite Elements in Analysis and Design 43(14):1039–1049, DOI 10.1016/j.finel.2007.06.006

Huang X, Xie YM (2009) Bi-directional evolutionary topology optimization of continuum structures with one or multiple materials. Computational Mechanics 43(3):393–401, DOI 10.1007/s00466-008-0312-0

Huang X, Xie YM (2010) Evolutionary topology optimization of continuum structures. John Wiley and Sons

Huang X, Xie YM, Burry MC (2006) A new algorithm for bi-directional evolutionary structural optimization. Japan Society of Mechanical Engineers International Journal Series C 49(4):1091–1099, DOI 10.1299/jsmec.49.1091

Liu Y, Jin F, Li Q, Zhou S (2008) A fixed-grid bidirectional evolutionary structural optimization method and its applications in tunnelling engineering. International Journal for Numerical Methods in Engineering 73(12):1788–1810, DOI 10.1002/nme.2145

Lund E, Stegmann J (2006) Eigenfrequency and buckling optimization of laminated composite shell structures using discrete material optimization. In: e MPB, Olhoff N, Sigmund O (eds) IUTAM Symposium on Topological Design Optimization of Structures, Machines and Materials, Springer Netherlands, vol 137, pp 147–156, DOI 10.1007/1-4020-4752-5_15

Nguyen T, Ghabraie K, Tran-Cong T (2014) Applying bi-directional evolutionary structural optimisation method for tunnel reinforcement design considering nonlinear material behaviour. Computers and Geotechnics 55:57–66, DOI 10.1016/j.compgeo.2013.07.015

Park J, Sutradhar A (2015) A multi-resolution method for 3d multi-material topology optimization. Computer methods in applied mechanics and engineering 285:571–586, DOI 10.1016/j.cma.2014.10.011

Querin OM, Steven GP, Xie YM (1998) Evolutionary structural optimisation (ESO) using a bidirectional algorithm. Engineering Computations 15(8):1031–1048, DOI

10.1108/02644409810244129
Querin OM, Victoria M, Díaz C, Martí P (2015) Layout optimization of multi-material continuum structures with the isolines topology design method. Engineering Optimization 47(2):221–237, DOI 10.1080/0305215X.2014.882332
Rispler A, Steven G (1995) Shape optimisation of metallic inserts in composite bolted joints. In: International Aerospace Congress 1995: Proceedings; Second Pacific International Conference on Aerospace and Technology; Sixth Australian Aeronautical Conference, Institution of Engineers, Australia, pp 225–229
Sigmund O, Petersson J (1998) Numerical instabilities in topology optimization: A survey on procedures dealing with checkerboards, mesh-dependencies and local minima. Structural and Multidisciplinary Optimization 16(1):68–75, DOI 10.1007/BF01214002
Sigmund O, Torquato S (1997) Design of materials with extreme thermal expansion using a three-phase topology optimization method. Journal of the Mechanics and Physics of Solids 45(6):1037–1067, DOI 10.1016/S0022-5096(96)00114-7
Stegmann J, Lund E (2005) Discrete material optimization of general composite shell structures. International Journal for Numerical Methods in Engineering 62(14):2009–2027, DOI 10.1002/nme.1259
Stolpe M, Svanberg K (2001) An alternative interpolation scheme for minimum compliance topology optimization. Structural and Multidisciplinary Optimization 22(2):116–124, DOI 10.1007/s001580100129
Tavakoli R (2014) Multimaterial topology optimization by volume constrained allen–cahn system and regularized projected steepest descent method. Computer Methods in Applied Mechanics and Engineering 276:534–565, DOI 10.1016/j.cma.2014.04.005
Tavakoli R, Mohseni SM (2014) Alternating active-phase algorithm for multimaterial topology optimization problems: A 115-line matlab implementation. Structural and Multidisciplinary Optimization 49(4):621–642, DOI 10.1007/s00158-013-0999-1
Thomsen J (1992) topology optimization of structures composed of one or two materials. Structural optimization 5(1–2):108–115, DOI 10.1007/BF01744703, presented at NATO ASI Optimization of Large Structural Systems, Berchtesgaden, Germany, Sept. 23 Oct. 4, 1991
Wang MY, Wang X (2004) "color" level sets: a multi-phase method for structural topology optimization with multiple materials. Computer methods in applied mechanics and engineering 193(6–8):469–496
Wang Y, Luo Z, Kang Z, Zhang N (2015) A multi-material level set-based topology and shape optimization method. Computer Methods in Applied Mechanics and Engineering 283:1570–1586, DOI 10.1016/j.cma.2014.11.002
Xie YM, Steven GP (1993) A simple evolutionary procedure for structural optimization. Computers & Structures 49(5):885–896, DOI 10.1016/0045-7949(93)90035-C
Yang XY, Xie YM, Steven GP, Querin OM (1999) Bidirectional evolutionary method for stiffness optimization. American Institute of Aeronautics and Astronautics Journal 37(11):1483–1488
Zhou M, Rozvany GIN (2001) On the validity of ESO type methods in topology optimization. Structural and Multidisciplinary Optimization 21(1):80–83, DOI 10.1007/s001580050170
Zhou S, Wang MY (2007) Multimaterial structural topology optimization with a generalized cahn–hilliard model of multiphase transition. Structural and Multidisciplinary Optimization 33(2):89–111, DOI 10.1007/s00158-006-0035-9